# Synchronized Symmetrical Bus-Clamping PWM Strategies for Three Level Inverter: Applications to Low Switching Frequencies

**Article** *in* International Journal of Emerging Electric Power Systems · January 2011

DOI: 10.2202/1553-779X.2722

CITATIONS
0

READS
83

**3 authors:**

Sreenivasappa Veeranna
Presidency University, Bangalore
**19** PUBLICATIONS **30** CITATIONS
SEE PROFILE

Udaykumar R Yaragatti
National Institute of Technology Karnataka
**166** PUBLICATIONS **1,017** CITATIONS
SEE PROFILE

A.R. Beig
Khalifa University
**92** PUBLICATIONS **1,013** CITATIONS
SEE PROFILE

# Synchronized SVPWM Algorithm for Overmodulation Region for Three-Level VSI

Sreenivasappa B Veeranna[*1] Udaykumar R Yaragatti[*] Abdul Rahiman Beig
[*]National Institute of Technology Karnataka, Surathkal, India
The Petroleum Institute, Abu Dhabi, UAE
sreebms@ieee.org udaykumarry@yahoo.com arbeig@ieee.org

***Abstract*- Synchronization is essential for the satisfactory operation of VSI in high power applications. With proper selection of switching states it is possible to obtain synchronization and symmetry in space vector pulse width modulation (SVPWM) algorithm. A novel SVPWM based switching algorithm, which results in improved *THD* and increased fundamental voltage in overmodulation region by maintaining synchronization and symmetry is presented in this paper. A simple method to determine the switching sequence to achieve synchronization, quarter wave symmetry, half wave symmetry and three phase symmetry in overmodulation region is presented. The proposed algorithm is simulated and its performance in terms of the *THD* and magnitude of fundamental voltage of output is studied in the overmodulation region. The results show the improved performance of the proposed algorithm compared to the existing algorithms. The proposed algorithm is verified experimentally on a constant *v/f* three level VSI fed induction motor drive.**

***Index Terms*- Harmonic distortion, Induction motor drives, Pulse width modulation, Pulse width modulated inverters, Synchronization.**

## I. INTRODUCTION

In high power drives, the switching frequency is very low, normally the pulse number *P,* (defined as the ratio of switching frequency ($f_s$) to the fundamental frequency ($f$)) is less than 21 [1-5]. In such cases, the synchronization is essential to avoid sub-harmonics. Synchronized sine-triangle pulse width modulation (SPWM) is widely used in industry in high power applications. It has been shown that, unlike SPWM, with SVPWM approach, it is not only possible to achieve synchronization but also possible to obtain half wave symmetry (HWS), quarter wave symmetry (QWS) and three phase symmetry (TPS) [3-5]. This is very useful, because at low *P*, lower harmonics are dominant and total harmonic distortion (*THD*) will be very low. With the symmetry, we can reduce the magnitude of the harmonics and improve the *THD*. The synchronized PWM for two-level inverter in linear modulation region is given in [3-4]. The synchronized SVPWM for three-level inverter in linear modulation is presented in [5]. No work has been reported on the operation of synchronized PWM in overmodulation region for three-level inverter. Even though overmodulation for two-level inverter is presented in [6], extending this to three-level is not straight forward. In this paper synchronized SVPWM operation has been extended to overmodulation region for three-level VSI. This is one of the major contributions of the present work.

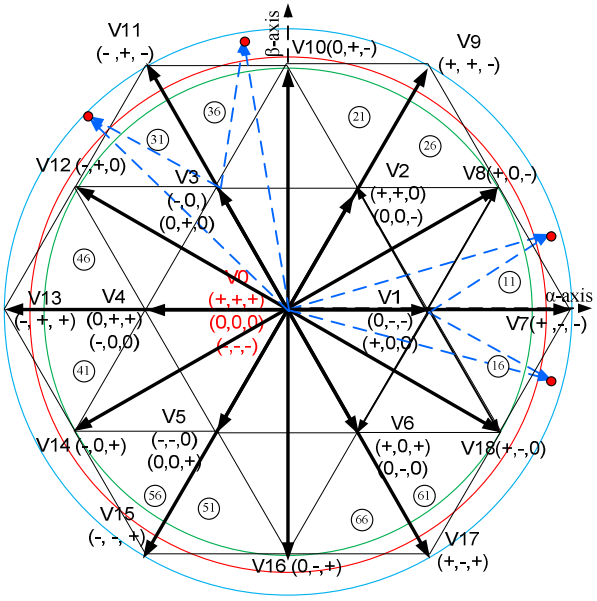


Fig.1. Switching vectors of three-level inverter in stationary reference frame.

Overmodulation operation is very useful in high power drives, as this gives *14%* additional utilization of dc bus [1-2]. Since three-level inverters are suitable for high power drives, the proposed algorithm will find application in industry. This paper presents the synchronized space vector PWM sequences for overmodulation region for three-level inverter. The synchronized PWM sequences for over modulation for three-level inverter are not reported in the literature. In the case of three-level inverter, the medium vectors (*V8, V10, V12, V14, V16* and *V18,* defined in fig 1.) also play a role in overmodulation region. These vectors are absent in two-level inverter. These medium vectors can be used in region-II of overmodulation. This is the novelty of the present work. Role of medium vectors makes the approach different from the two–level synchronized PWM sequences. The SVPWM for over modulation for high switching frequency for three-level inverter is reported in the literature [7-10]. In [7-10], the conventional two-level SVPWM approach for over modulation has been extended to three level inverters and medium vectors are not considered. The present work is an improvement over it and results in improved performance

The synchronized switching pulses for overmodulation region have been explained in this paper. The proposed algorithm is illustrated through MATLAB simulation. The results are validated experimentally. It is shown that, the proposed approach, results in increased fundamental voltage ($V_f$) and improved *THD* compared to the conventional two-level approach presented in [7-10].

[1] Sreenivasappa B Veeranna is currently a visiting graduate research assistant at Electrical Engineering Department, The Petroleum Institute, Abu Dhabi, UAE.

978-1-4244-5226-2/10/$26.00 ©2010 IEEE

The principles of the synchronized PWM have been reviewed briefly in section II. The synchronized SVPWM for three-level inverter in overmodulation region is explained in section III. Simulation results are presented in section IV. The performance of the proposed switching algorithm is studied in terms of weighted total harmonic distortion of the line voltage ($V_{LWTHD}$) and magnitude of fundamental voltage for all the possible value of $P$ in entire overmodulation region. The experimental results are given in section V.

## II. Synchronized SVPWM for Three-Level Inverter

The basic principles of SVPWM to maintain synchronization , quarter wave symmetry (QWS), half wave symmetry (HWS) and three phase symmetry (TPS) for three level inverters are given in[5]. The same basic principles are extended to overmodulation region and hence a brief review of synchronized SVPWM for three-level inverter is discussed in this section. A three-level inverter has $3^3$=27 switching states. The space vector diagram of inverter states are shown in fig.1. There are 24 active states (6 Large vectors (*V7[+--]*, *V9[++-]*, *V11[-+-]*, *V13[-++]*, *V15[--+]* and *V17[+-+]*), 6 Medium vectors, 12 Small vectors (*V1[+00, 0--]*, *V2[++0, 00-]*, *V3[0+0, -0-]*, *V4[0++, -00]*,

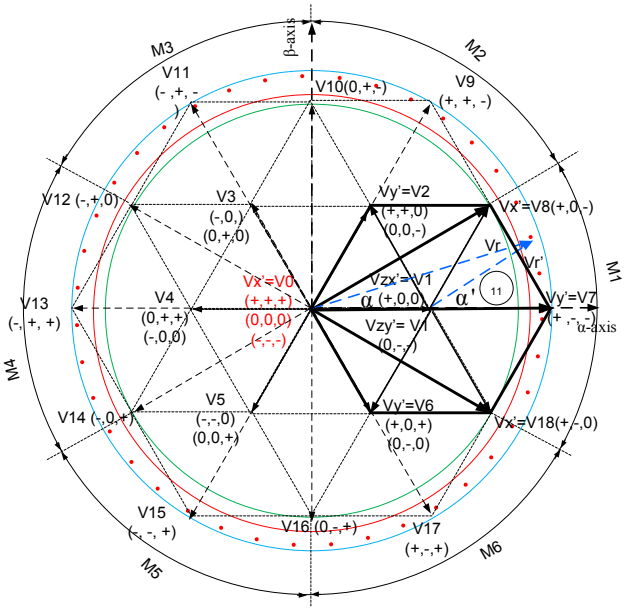


F ig. 2. Space vector diagram of three-level inverter in overmodulation region.

*V5[00+, --0]* and *V6[+0+, 0-0]*) and three zero vectors *V0 [+++, 000, ---]*. These are defined in fig. 1, + means the phase is connected to positive dc bus, - indicates the phase is connected to negative dc bus and 0 indicates the phase is connected to middle point of the dc bus.

A simple synchronized PWM sequence should have following characteristics.

A. Minimum possible switching frequency.

B. Output voltage should be synchronized with reference.

C. Should have HWS, QWS and TPS.

### A. *Conditions for minimum switching frequency:*

- Only one switching per phase is allowed in each sample.
- There should not be switching from one sample to another.

### B. *Conditions for synchronization and symmetry*

The necessary and sufficient conditions to achieve synchronization, HWS, QWS and TPS [5] are summarized in table I. $S_A$, $S_B$, $S_C$ are the switching states of phase A, phase B and phase C respectively. The complementary state is indicated by a prime ('), which means complementary state of + is - and vice versa and the complementary state of state 0 is 0.

### C. *Synchronized SVPWM for Overmodulation Region*

Inverter states can be chosen to design switching sequences that satisfy above conditions resulting in minimum switching as well as maintain synchronization and various symmetries. The inverter states and the corresponding space vectors of three-level inverter in stationary reference frame are shown in fig. 1. The space vector plane can be divided into six major sectors (*M1 to M6*) of 60 degree interval. The space vectors of each of the major sector constitute a hexagonal with small vectors (*V1* to *V6*) at the center. It should be noted that in the overmodulation region, one of the small vectors (*V1* to *V6*)

TABLE I
Conditions of Synchronization, HWS, QWS, and TPS

| | Synchronization | HWS | QWS | TPS | TPS |
|---|---|---|---|---|---|
| Inverter state at $\theta$ | Inverter state at $2\pi \pm \theta$ | Inverter state at $\pi \pm \theta$ | Inverter state at $\pi/2 \pm \theta$ | Inverter state at $2\pi/3 + \theta$ | Inverter state at $2\pi/3 - \theta$ |
| $S_A$ | $S_A$ | $S'_A$ | $S_A$ | $S_C$ | $S_B$ |
| $S_B$ | $S_B$ | $S'_B$ | $S_B$ | $S_A$ | $S_C$ |
| $S_C$ | $S_C$ | $S'_C$ | $S_C$ | $S_B$ | $S_A$ |

is one of the nearest three vectors and this keeps changing in each of the major sectors. This results in one additional switching when the sample moves form one major sector to another major sector. This additional switching results in narrow switching pulse, which may not be possible to implement practically. To avoid this narrow switching pulse, the switching sequence of the last sample in current major sector is stopped on a switching state which is common with the next major sector. The first sample of the next sector starts from this switching state.

The switching states for *N=4* and *N=5* in major sector 1 are given table II and III respectively. $T_{zx}$, $T_x$, $T_y$ and $T_{zy}$ are the dwell times of the switching vectors defined in subsection D. The last sample in major sector 1 is stopped at switching state *V8 [+,0,-]* which is common to major sector 1 and 2. So the switching sequence for the first sample in major sector 2 will start with *V8 [+, 0,-]*.

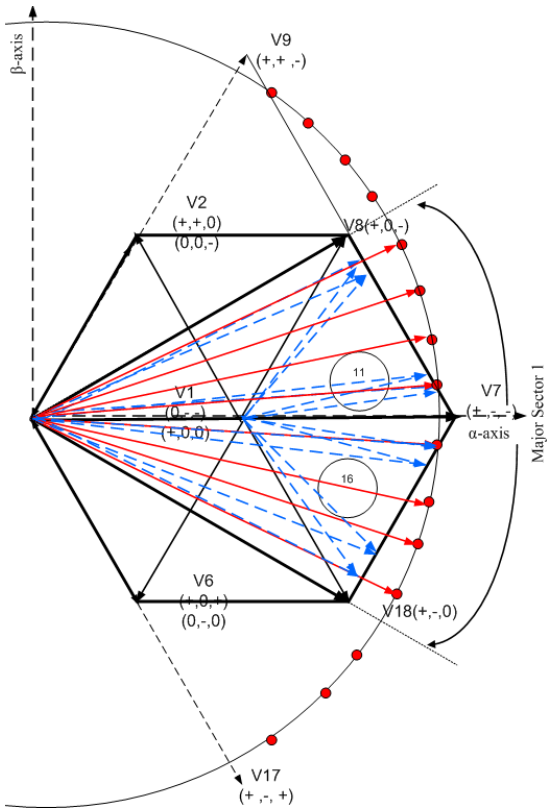


Fig.3. Vectors for $N$=8 (red lines before and blue lines after premodulation)

Let $N$ be the number of samples per sector. Even $N$ will have switching sequences similar to $N$=4 and odd $N$ will have switching sequences similar to $N$=5. For $N$=4, 4 samples are equally spaced in 60 degree interval which results in first two samples in subsector 6 and next two samples are in subsector 1. For $N$=5, five samples are equally spaced in 60 degrees interval which results in first two equally spaced samples in sub-sector 6, the third sample on the boundary between these two subsectors and last two samples in subsector 1 and. For third sample the dwell time of the small vector is zero. The switching sequence for $N$=4 and $N$=5 is given table II and table III respectively.

TABLE II
SWITCHING SEQUENCE FOR $N$ = 4 SAMPLES/SECTOR

| Triangle No. | Sample No. | Dwell times | | | |
|---|---|---|---|---|---|
| | | $T_{zx}$ | $T_x$ | $T_y$ | $T_{zy}$ |
| 16 | 1 | + - 0 | + - - | + - 0 | + 0 0 |
| 16 | 2 | + 0 0 | + - 0 | + - - | 0 - - |
| 11 | 3 | 0 - - | + - - | + 0 - | + 0 0 |
| 11 | 4 | + 0 0 | + 0 - | + - - | + 0 - |

TABLE III
SWITCHING SEQUENCE FOR $N$ = 5 SAMPLES/SECTOR

| Triangle No. | Sample No. | Dwell times | | | |
|---|---|---|---|---|---|
| | | $T_{zx}$ | $T_x$ | $T_y$ | $T_{zy}$ |
| 16 | 1 | + - 0 | + - - | + - 0 | + 0 0 |
| 16 | 2 | + 0 0 | + - 0 | + - - | 0 - - |
| 11 | 3 | 0 - - | + - - | + - - | 0 - - |
| 11 | 4 | 0 - - | + - - | + 0 - | + 0 0 |
| 11 | 5 | + 0 0 | + 0 - | + - - | + 0 - |

From the conditions given in Table I above, it can be derived that the switching sequences of one major sector is related to the switching sequences of next major as in (1).

$$S_A(\theta+\frac{\pi}{3}) = S'_B(\theta)$$
$$S_B(\theta+\frac{\pi}{3}) = S'_C(\theta) \quad (1)$$
$$S_C(\theta+\frac{\pi}{3}) = S'_A(\theta)$$

This is very useful relation. If the switching sequences of one major sector are derived to satisfy the conditions of synchronization and symmetry, then the sequences for the entire cycle can be computed using (1).

### D. *Calculation of Dwell Times*

The complexity of three-level SVPWM can be simplified by grouping the space vector of three-level inverter into six major sectors with small vectors at the centre [5]. With this approach, in each major sector, the vectors appear to be similar to that of two-level inverter. Each major sector can be divided into six sub-sectors. For example, the major sector 1 is divided into six subsectors from 11 to 16, shown in solid lines in fig. 2. The small vector at the origin, all the other active vectors will have 0.5p.u. magnitude as shown in fig. 2. The reference vector $V_r$ is sampled at regular intervals at $T_s$ and the reference magnitude of all vector appear as $V'_r$ at an angle $\alpha'$ as shown in fig. 2.

In overmodulation, only the tip of the $V_r$ belongs to sub-sectors 1 and 6. Hence only these two subsectors are of interest for the present work. The dwell times ($T_x$, $T_y$ and $T_z$) for subsectors 1 and 6 are calculated using (2) and (3) respectively, and due to symmetry these equations are valid for all the major sectors.

$$T_x = 2.309V'_{r\beta}T_s$$
$$T_y = (2V'_{r\alpha} - 1.1547V'_{r\beta})T_s \quad (2)$$
$$T_z = T_s - (T_x + T_y)$$
$$T_{zx}=T_{zy} = T_z/2,$$

where $T_s$ is the sampling period.

$$T_x = -2.309V'_{r\beta}T_s$$
$$T_y = (2V'_{r\alpha} + 1.1547V'_{r\beta})T_s \quad (3)$$
$$T_z = T_s - (T_x + T_y)$$

## III. MODULATION INDEX AND OVERMODULATION REGION

For a given dc bus voltage ($V_{DC}$), the modulation index ($M_i$) is defined as the ratio of the fundamental voltage generated to the fundamental voltage corresponding to six-step operation [3, 5, 10, 11]. In linear modulation range ($0 \le M_i < 0.907$) the tip of the average vector generated has a circular trajectory of radius $V_r$ as shown by the inner circle in fig. 2. In this region the $M_i$ is linearly related to the $V_r$. The region ($0.907 < M_i \le 1$) between the inner most circle and outmost circle in fig. 2 is defined as overmodulation region. In this region, the reference circle is partly outside and partly within the hexagon. The inverter cannot generate an average vector, whose tip falls outside the hexagon. Premodulation is required to correct these samples and to synthesize the desired reference. This results in reduced fundamental voltage and hence the relation between $M_i$ and $V_r$ is not linear [3]. In two-level inverter the overmodulation

region is divided into two zones, namely overmodulation region I ($0.907< M_i \leq 0.952$) and overmodulation region II ($0.9532 < M_i \leq 1$). The same region I and region II region definition is extended to three-level inverter in [7-12] as the medium vectors are not considered. In the present work the medium vectors are also considered and with this approach the overmodulation region I is valid only in the region ($0.907< M_i \leq 0.92$) and rest of the region can be classified as overmodulation region II ($0.92< M_i \leq 1$).

*Premodulation*

In overmodulation region-I , only the magnitude is corrected for the samples which fall outside the hexagon as in (4).

$$\begin{aligned} V'_{rp} &= V'_r \quad \text{if } V'_r \leq V'_{rm} \\ &= V'_{rm} \quad \text{if } V'_r > V'_{rm} \end{aligned}$$

$$V'_{rm} = \frac{0.433}{\cos(30^0 - \propto')}$$

$$\propto'_c = \propto' \qquad (4)$$

This approach increases the $M_i$ beyond 0.907.

In overmodulation region-II the modulation index is increased by shifting the average vectors generated closer to their nearest sub-sector boundaries. In fig. 3, the samples which are closer to *V7* in sub-sector 11 are moved towards vector *V7* and the samples which are closer to *V8* are pushed towards medium vector *V8*. Similarly in subsector 16, the samples which are closer to *V7* are moved towards vector *V7* and those vectors closer to medium vector *V18* are pushed towards medium vector *V18*. This is achieved by the amplitude and angle correction using (5)

$$\begin{aligned} \propto'_c &= \propto_a \propto' \quad \text{if } 0^0 \leq \propto' < 30^0 \\ &= 30^0 \quad \text{if } \propto' = 30^0 \\ &= 60^0 - \alpha_a (60^0 - \propto') \quad \text{if } 30^0 < \propto' < 60^0 \qquad (5) \end{aligned}$$

$$V'_{rm} = \frac{0.433}{\cos(30^0 - \propto'_c)}$$

This is different from the existing methods [7-10]. In [7-10] all samples in subsector 11 and subsector 16 are pushed towards *V7, V8* and *V18* are not considered.

## IV. SIMULATION RESULTS AND PERFORMANCE ANALYSIS

Synchronized PWM strategies for three-level inverter are simulated using MATLAB/SIMULINK and applied to a *v/f* drive consists of a 440V, 3.75KW, 1450rpm, three phase rpm induction motor powered from a three level IGBT based inverter.

The simulation waveforms of pole voltage ($V_{AO}$), defined as the voltage between output terminal and the dc mid-point, line voltage ($V_{AB}$) and no load motor current ($i_A$) , are given in fig 4 and fig.6 for $N$=4 in overmodulation region I and region II respectively. Their corresponding harmonic spectrums (excluding fundamental components) are given in fig 5 and 7.

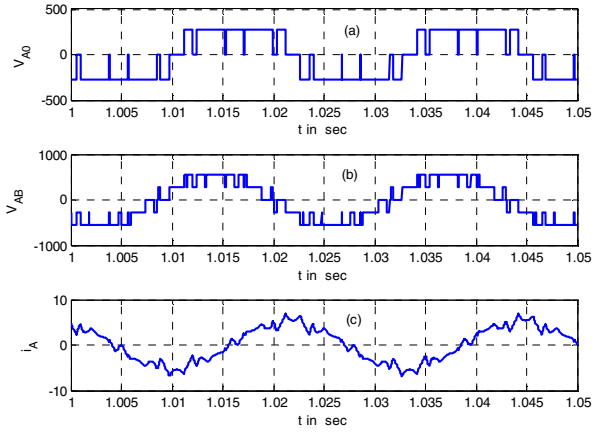


Fig. 4. Waveforms of (a) Pole voltage $V_{AO}$ (b) Line voltage $V_{AB}$ (c) Current $i_A$ for $N$=4 in overmodulation region-I at $Mi$=0.91

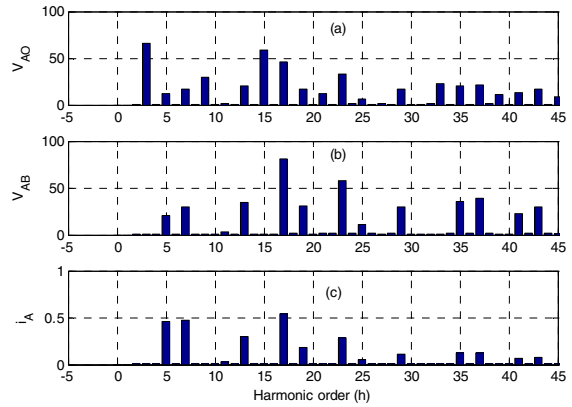


Fig. 5. Harmonic Spectrum (excluding fundamental) of (a) Pole voltage $V_{AO}$ (b) Line voltage $V_{AB}$ (c) Current $i_A$ for $N$=4, in overmodulation region-I at $M_i$=0.91.

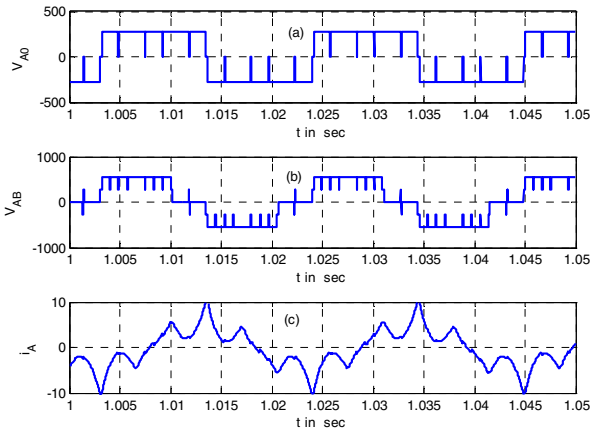


Fig. 6. Waveforms of (a) Pole voltage $V_{AO}$ (b) Line voltage $V_{AB}$ (c) Current $i_A$ for $N$=4 in overmodulation region-II at $Mi$=0.98

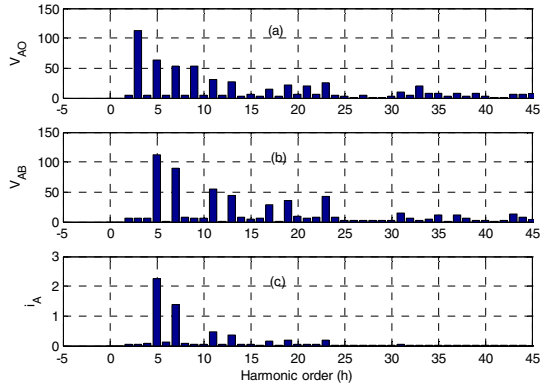


Fig. 7. Harmonic Spectrum (excluding fundamental) of (a) Pole voltage $V_{AO}$ (b) Line voltage $V_{AB}$ (c) Current $i_A$ for $N$=4 in overmodulation region-II at $M_i$=0.98.

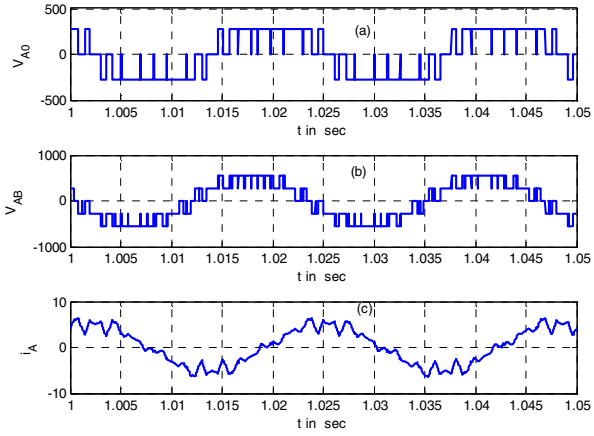


Fig. 8. Waveforms of (a) Pole voltage $V_{AO}$ (b) Line voltage $V_{AB}$ (c) Current $i_A$ for $N$=7 in overmodulation region-I at $Mi$=0.91.

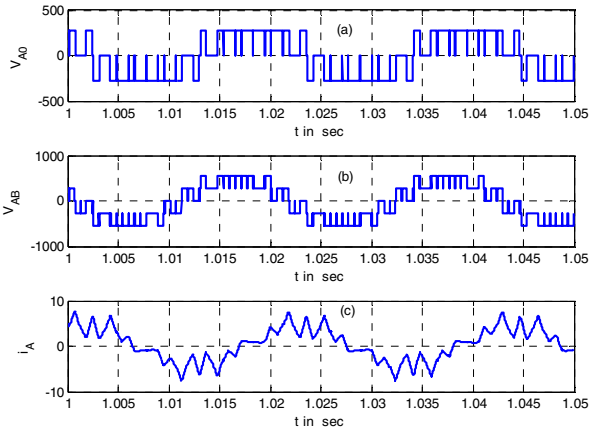


Fig. 10. Waveforms of (a) Pole voltage $V_{AO}$ (b) Line voltage $V_{AB}$ (c) Current $i_A$ for $N$=7 in overmodulation region-II at $M_i$=0.98.

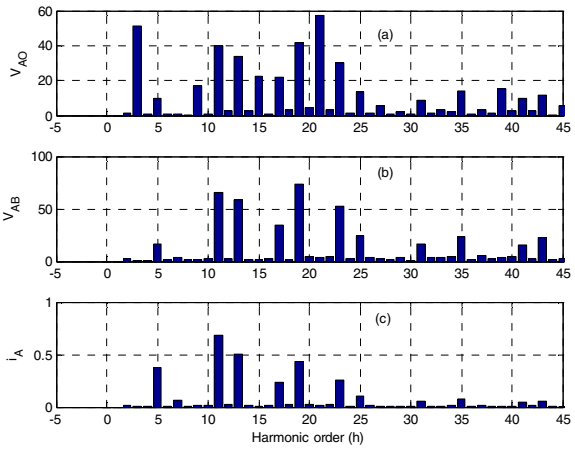


Fig. 9. Harmonic Spectrum (excluding fundamental) of (a) Pole voltage $V_{AO}$ (b) Line voltage $V_{AB}$ (c) Current $i_A$ for $N$=7, in overmodulation region-I at $M_i$=0.91.

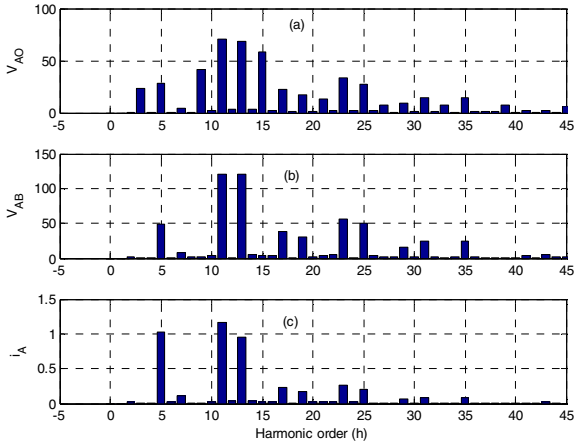


Fig. 11. Harmonic Spectrum (excluding fundamental) of (a) Pole voltage $V_{AO}$ (b) Line voltage $V_{AB}$ (c) Current $i_A$ for $N$=7 in overmodulation region-II at $M_i$=0.98.

TABLE IV
FUNDAMENTAL COMPONENTS AND *THD* OF THE POLE VOLTAGE, LINE VOLTAGE AND MOTOR CURRENT

| | | Fundamental Components | | | Weighted *THD* & *THD* | | |
|---|---|---|---|---|---|---|---|
| $N$ | $M_i$ | $V_{AO1}$ | $V_{AB1}$ | $i_{A1}$ | $V_{WTHD}$ | $V_{LWTHD}$ | $I_{THD}$ |
| 4 | 0.91 | 330V | 574V | 4.6A | 0.0544 | 0.0142 | 0.1920 |
| 4 | 0.98 | 343V | 595V | 5A | 0.0914 | 0.0387 | 0.5429 |
| 7 | 0.91 | 300V | 550V | 5A | 0.0445 | 0.0162 | 0.2158 |
| 7 | 0.98 | 310V | 560V | 5.15A | 0.0406 | 0.0304 | 0.4103 |

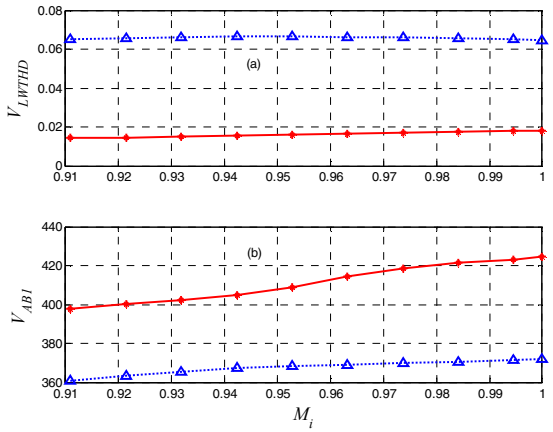


Fig. 12. Plots of (a) $V_{LWTHD}$ v/s $Mi$ (b) line voltage v/s $Mi$, red solid line (proposed method considering medium vectors), blue dotted line (existing method without considering medium vectors)

Similarly the waveforms for $N$=7 are given in fig 8 and fig. 10 for overmodulation region I and II respectively. Their corresponding harmonic spectrum (excluding fundamental components) is given in fig. 9 and fig. 11. The fundamental components and weighted *THD* of the pole voltage, line voltage along with fundamental component and *THD* of the motor current are given in table IV.

The waveforms exhibit perfect synchronization and symmetry. The FFT plots demonstrate the absence of even harmonics which proves *HWS*. The triplen harmonics are present in the pole voltage (plot (a) in fig 5, fig 7, fig.9 and fig.11) and they are cancelled in line voltage (plot (b) in fig 5, fig 7, fig.9 and fig.11) and motor current (plot (c) in fig 5, fig 7, fig.9 and fig.11), due to TPS. The $V_{LWTHD}$ and $V_{AB1}$ for the entire overmodulation region are plotted in fig.12 and this result is compared with the methods given in [7-10]. It is observed that the proposed method results in better $V_{LWTHD}$ and higher $V_{AB1}$. The performance of the proposed SVPWM with or without symmetry consideration is studied. In both the cases synchronization is maintained. The comparative

results are given in fig 13. As expected, the symmetry in the proposed SVPWM algorithm reduces the *THD* significantly.

## V. EXPERIMENTAL IMPLEMENTATION

The above synchronized SVPWM algorithm is implemented on a DSP based digital controller. The event manager module is initialized with the initial switching vector. The switching sequence started with the zero-crossing point of the reference vector. Hence the starting vector is *V16 [0 - +]*.The event manager is programmed to compute the next state and the sequences are automatically generated by the event manager. Even though it is possible to generate sequences for the entire cycle of the reference vector, there may be cases where there will be sudden change in reference vector position. In order to take care of this situation, the starting vectors of all the major sectors are stored, thus only six vectors namely *V16, V18, V8, V10, V12* and *V14* need to be stored and rest of the sequences are determined by the event manager.

The algorithm is being verified on a constant *v/f* drive. A

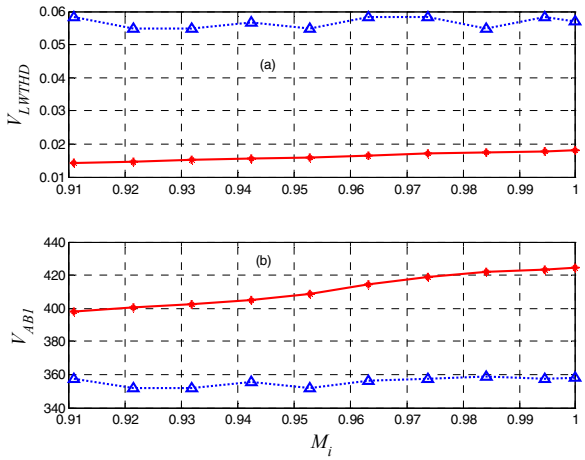


Fig. 13. Plots of (a) $V_{LWTHD}$ v/s *Mi* (b) line voltage v/s *Mi*, red solid line (proposed method - Synchronization with symmetry), blue dotted line (proposed method - Only synchronization, no symmetry).

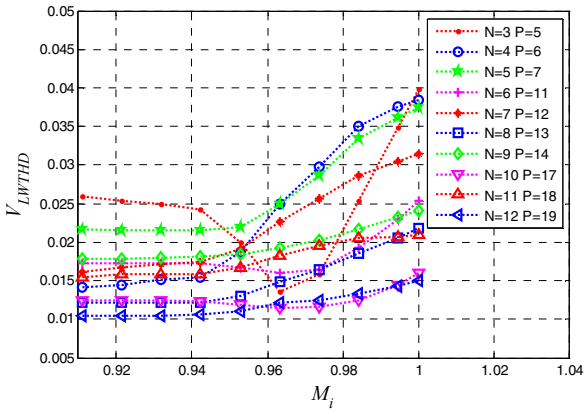


Fig. 14. line *THD* v/s $M_i$ for *N*=3 to12.

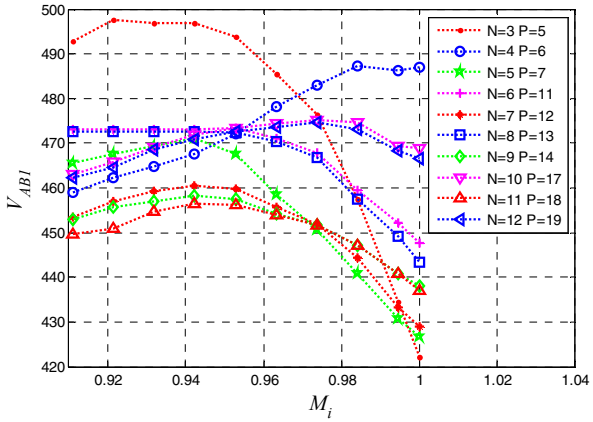


Fig. 15. line voltage v/s $M_i$ for N=3 to 12

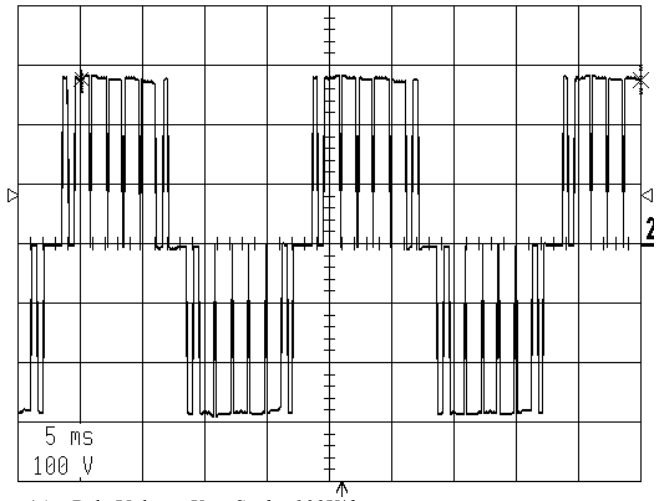


*(a)* Pole Voltage $V_{AO}$ , *Scale: 100V/div*

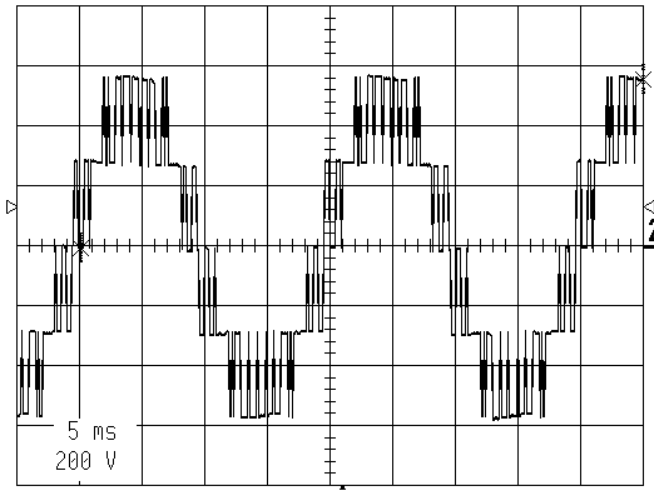


*(b)* Line Voltage $V_{AB}$ , *Scale : 100V/div*

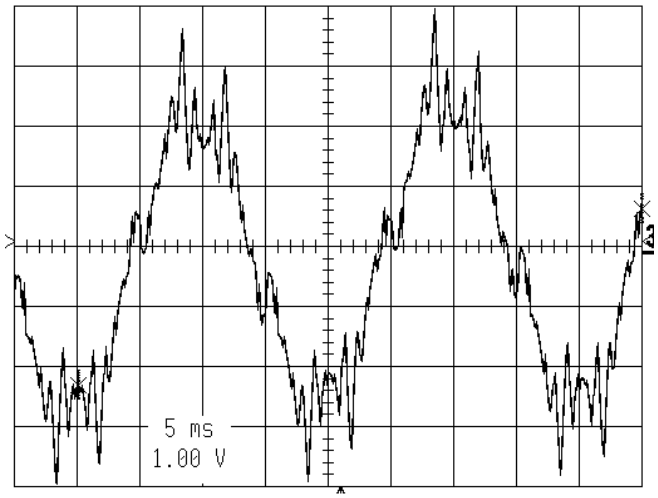


*(c)* Motor no load current $i_A$ , *Scale: 2.5A/div*

Fig 16. Experiemtnal results : *N*=7, $M_i$=0.98(region II).

440v, 3.75KW, 3Φ, 50Hz, 1450 rpm, induction motor is used in the experimental prototype. The drive will pass through linear region ($0 < M_i \leq 0.907$) and the synchronized SVPWM sequence given in given in [5] are used for this region and the proposed switching sequence is used in the overmodulation region. The experimental tests are in progress, typical experimental waveform for $N$=7 at $M_i$=0.98 are given in fig. 16. More experiments need to be carried out to study the effect of DC bus voltage on the waveform and harmonics.

## VI. CONCLUSIONS

A synchronized and symmetrical SVPWM algorithm for overmodulation region for three-level inverter has been presented. In the proposed algorithm higher DC bus utilization is achieved. The performance is compared with the existing methods. It is shown that the performance of the proposed algorithm is better in terms of *THD* and dc bus utilization compared to existing methods. The proposed three-level synchronized switching algorithm has applications in medium voltage high power drives. This will be useful in slow start of high power motors, where *v* and *f* can be changed in every major sector to achieve synchronization and symmetry and the same time *v/f* ratio can be maintained constant. Compared to conventional synchronized SPWM all possible values of pulse number are achieved in the proposed method. This results in smooth operation of the motor even in the overmodulation region.

## REFERENCES


[1] Bimal K. Bose, "Power Electronics and Motor Drives, Advances and Trends" Academic Press, 2006.

[2] H. Stemmler, P. Guggenbeck "High power industrial drives", *Proceedings of IEEE*, vol82 (8), pp 1266-1286, Aug.1994.

[3] Marchesoni, M.; Mazzucchelli, M.; Multilevel converters for high power AC drives: a review" in Proc. *IEEE International Symposium on Industrial Electronics, ISIE'93* , vol.1, pp.38 -43, 1993.

[4] G. Narayanan, V. T. Ranganathan, "Synchronized PWM strategies based on space vector approach. Part 1: Principle of waveform generation," IEE Proc-Electr. Power Appl., vol. 146, No. 3, pp. 267-275, May 1999.

[5] A. R. Beig, G. Narayanan, and V. T. Ranganathan, "Modified SVPWM Algorithm for Three Level VSI With Synchronized and Symmetrical Waveforms," IEEE Transactions on Industrial Electronics, vol. 54, pp. 486–494, February 2007.

[6] G. Narayanan, V. T. Ranganathan, "Extension of Operation of Space Vector PWM Strategies with Low Switching Frequencies Using Different Overmodulation Algorithm" IEEE Trans. PE, vol. 17, pp. 788-798, 2002.

[7] C.Cecati, A. Dell'Aquila, A. Lecci, M. Liserre, V.G. Monopoli, "A discontinuous carrier-based multilevel modulation for multilevel converters," 3$^{0th}$ Annual Conference of IEEE Industrial Electronics Society, IECON 2004, vol1, pp 280-285, 2004.

[8] Ojo, Kshirsagar," The generalized discontinuous PWM modulation scheme for three-phase voltage source inverters, " The 29th Annual Conference of the IEEE Industrial Electronics Society, IECON '03, Vol. 2, pp 1629 – 1636, 2003

[9] S. K. Mondal, B. K. Bose, V. Oleschuk, J. O. P. Pinto,"Space Vector Pulse Width Modulation of Three-Level Inverter Extending Operation into Overmodulation Region" IEEE Trans. PE, vol. 18, pp. 604-610, 2003.

[10] A. K. Gupta, A. M. Kambadkone, "A General Space Vector PWM Algorithm for Multi-level Inverters, Including Operation in Overmodulation range" IEEE Trans. PE, vol. 22, no. 2, pp. 517-526, 2007.

[11] A. K. Gupta, A. M. Kambadkone, "A General Space Vector PWM Algorithm for Multi-level Inverter, Including Operation in Overmodulation range " International Electric Machines and Drives Conference, pp. 2527-2533, 2005.

[12] A. Tripathi, A. M. Kambadkone, S. K. Panda, "Direct method of overmodulation with integrated closed loop stator flux vector control" IEEE Trans. PE, vol20, no. 5, pp. 1161-1168, 2005.